Calcium sparks and calcium homeostasis in a hybrid model of local and global calcium responses

Jana M. Hartman
Advisor: Gregory D. Smith

Abstract

Intracellular free calcium (Ca^{2+}) signaling in cardiac myocytes has been studied extensively through both experiments and modeling. Of particular interest are the changes in bulk Ca^{2+} concentration in the cytosol and endoplasmic reticulum (ER) and the dynamics of localized Ca^{2+} elevations due to Ca^{2+} release from clusters of Ca^{2+}-regulated ion channels. This paper develops a hybrid whole cell model that accounts for both of these spatial scales of Ca^{2+} signaling and examines the effect of stochastic Ca^{2+} release (i.e. Ca^{2+} sparks) on whole cell Ca^{2+} homeostasis. When used to simulate experimental studies that examined the effects of tetracaine and flecainide on local and global Ca^{2+} signaling, the model behaves consistently with experiments and supports the qualitative explanations of experimental results that appeared in Zima et al. *Biophys. J.* 94(5): 1867, 2008.

1 Introduction

Intracellular free calcium (Ca^{2+}) concentration is an important cellular signal whose dynamics are controlled through several mechanisms, including ion channels on the endoplasmic reticulum (ER) membrane. These intracellular Ca^{2+} channels are regulated by the binding of cytosolic Ca^{2+} which can activate and inactivate them. The two major classes of such intracellular Ca^{2+} channels, inositol 1,4,5 trisphosphate receptors (IP_3Rs) and ryanodine receptors (RyRs), are often clustered together in Ca^{2+} release sites small enough to be coupled by increases in cytosolic Ca^{2+} concentration on a spatial scale of 50-500 nanometers. The stochastic opening of a few such channels, and the resulting release of Ca^{2+} from the ER, can cause a larger number of the channels in the release site to open. These concerted openings are known as Ca^{2+} puffs or sparks.

Most previous theoretical research on spark statistics has focused on models of individual channels and release sites, and on the relationship between channel kinetics and puff/spark dynamics. In prior work, the Ca^{2+} concentration in the subspace directly around the channel is often modeled as a variable that changes with channel opening, while the bulk cytosolic and ER Ca^{2+} concentrations are parameters that provide boundary conditions for the system [1–4]. Other studies that focus on whole cell Ca^{2+} dynamics usually use a Hodgkin-Huxley type gating variable that represents opening and closing of a large number of IP_3Rs or RyRs that are evenly distributed along the ER membrane [5–7]. In contrast, this paper presents a

hybrid whole cell model that accounts for both local and global aspects of Ca^{2+} signaling by coupling a compositionally defined Markov chain to nonlinear ODEs. We use this model to examine the effect of the RyR inhibitors on Ca^{2+} release site statistics and whole cell Ca^{2+} homeostasis.

Understanding the dynamics of Ca^{2+} release via sparks is particularly important in the study of heart muscle, where changes in patterns of local Ca^{2+} signaling play a role in cardiac arrhythmias. Experimental work [8,9] has shown that tetracaine, a local anaesthetic, reduces the open probability of individual RyRs by increasing the dwell time in a closed state. When added to cardiac myocytes, tetrcaine also causes an unexpected result of prolonged spark duration. The authors suggested that this counter-intuitive result is due to an increased Ca^{2+} load in the ER caused by the observed decrease in spark frequency, which may allow the ER to release more Ca^{2+} when sparks do occur. The initial goal of this research was to determine if this result can be reproduced in a whole cell model that accounts for the effect to stochastic Ca^{2+} release (i.e. sparks) on whole cell Ca^{2+} homeostasis, thereby demonstrating the consistency of the hypothesis presented in Zima et al.

Experiments have also shown that flecainide causes a similar reduction in open probability of individual RyRs, but by a different mechanism than tetracaine [8–10]. Experimental evidence suggests that tetracaine increases the dwell time in closed states, and most authors agree that tetracaine has no effect of the open state dwell time (for an exception see [10]). In contrast, flecainide decreases the open dwell time of RyRs, while leaving the closed dwell time constant [10]. The hybrid model of local and global Ca^{2+} signaling presented here provides an opportunity to examine how these pharmacological agents that reduce the open probability of single channels may interact to effect spark dynamics involving clusters of coupled RyRs and whole cell Ca^{2+} homeostasis.

2 Model Formulation

2.1 Overview

The hybrid Markov Chain-ODE model developed here takes into account both the release site dynamics and the homeostasis of the whole cell Ca^{2+} (Fig. 1). The model assumes that intracellular Ca^{2+} channels are clustered on the ER membrane in release sites composed of 10-100 channels. We assume that when a release site changes state, the local Ca^{2+} concentration around the release site changes faster than the bulk concentrations. Therefore, the model includes local domains on both the cytosolic and luminal sides of the membrane with concentrations dependent on their respective bulk concentrations and the number of open channels in the release site. The release sites are coupled to the bulk concentrations, allowing changes in the release sites to affect the bulk cytosolic and ER Ca^{2+}. Additionally, a flux is added to account for the action of the SERCA pumps, which re-sequester Ca^{2+} in the ER after release into the cytosol. A passive leak from the ER to the cytosol allows for movement of Ca^{2+} from the ER even when no channels are open.

In the experimental studies of Ca^{2+} dynamics that are the focus of this work, the cells are permeabilized; that is, a pharmacological agent has been added to the bath that perforates the cell membrane. This effectively clamps the cytosolic Ca^{2+} concentration at the level of the bathing solution. The plasma membrane fluxes represented in the model allow for

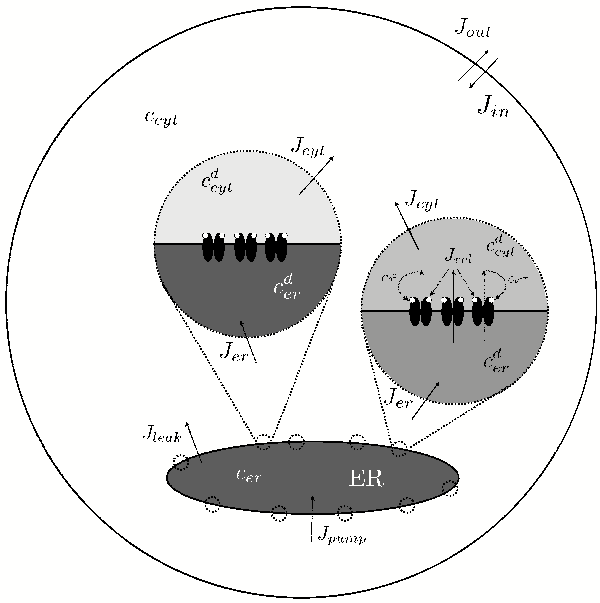

Figure 1: The hybrid whole cell model represents two bulk compartments: the ER (c_{er}) and the cytosol (c_{cyt}). The membrane of the ER includes multiple release sites, each of which includes a local Ca^{2+} domain on both sides of the membrane. The release sites are independent, stochastic units; two release sites in different states are shown. The domain Ca^{2+} concentrations (c^d_{cyt} and c^d_{er}) are influenced by fluxes that involve the bulk Ca^{2+} concentrations (cytosolic and ER) and the state of the release site. Fluxes include diffusion from cytosolic domains to the bulk cytosol (J_{cyt}), diffusion from the bulk ER to the luminal domains (J_{er}), the SERCA pump flux that re-sequesters Ca^{2+} into the ER (J_{pump}), a passive leak from the ER to the cytosol (J_{leak}), and the fluxes across the plasma membrane (J_{in} and J_{out}).

modeling an intact cell (when the values are low) or a permeabilized cell (when the fluxes are high).

2.2 Ca^{2+} release site model

The basic unit of the hybrid model is a single channel model of a Ca^{2+}-regulated intracellular Ca^{2+} channel. There are many such single channel models in the literature, ranging in complexity from two to several hundred states. The simplest possible single channel RyR model includes two states, closed (C) and open (O). The RyR opens at a rate dependent on the local Ca^{2+} concentration and closes with a constant (i.e. Ca^{2+}-independent) transition rate,

$$C \underset{k^-_{21}}{\overset{k^+_{12}c^\eta}{\rightleftharpoons}} O, \tag{1}$$

where η is the cooperativity of Ca^{2+} binding, c is the local [Ca^{2+}], $k^+_{12}c^\eta$ and k^-_{21} are transition

rates with units of reciprocal time, and k_{12}^{+} is an association rate constant with units of $\text{conc}^{-\eta}\text{time}^{-1}$. If the local $[Ca^{2+}]$ is specified, the transition state diagram (Eq. 1) defines a discrete-state continuous-time stochastic process, $S(t)$, that takes on values in the state-space $\mathcal{S} = (C, O)$.

In order to incorporate this single channel RyR model into a Ca^{2+} release site model, we assume that the release site is composed of N stochastically gating channels. We also assume mean-field coupling; the local $[Ca^{2+}]$ experienced by a channel depends only on the bulk concentrations c_{cyt} and c_{er} and the number of open channels at the Ca^{2+} release site, not the spatial arrangement of those channels. The state space for the Ca^{2+} release site model thus includes $(N+1)$ states given by $\mathcal{S} = ((N,0),(N-1,1),(N-2,2)...(1,N-1),(0,N))$, where $(N_C,\ N_O)$ indicates the number of closed and open channels, respectively.

The transition-state diagram for a release site composed of N channels is shown below, where the local $[Ca^{2+}]$ used in each Ca^{2+}-mediated transition is indicated by c_n, with $0 \leq n \leq N$ indicating the number of open channels.

$$\begin{array}{ccccccccccc} & & Nk_{12}^{+}c_0^{\eta} & & (N-1)k_{12}^{+}c_1^{\eta} & & (N-2)k_{12}^{+}c_2^{\eta} & & 2k_{12}^{+}c_{N-2}^{\eta} & & k_{12}^{+}c_{N-1}^{\eta} & \\ 0 & \rightleftharpoons & 1 & \rightleftharpoons & 2 & \rightleftharpoons & \cdots & \rightleftharpoons & N-1 & \rightleftharpoons & N \\ & & k_{21}^{-} & & 2k_{21}^{-} & & 3k_{21}^{-} & & (N-1)k_{21}^{-} & & Nk_{21}^{-} & \end{array} \tag{2}$$

The resulting Q-matrix corresponding to (Eq. 2) is

$$Q = q_{ij} = \begin{pmatrix} \diamond & Nk_{12}^{+}c_0^{\eta} & 0 & 0 & 0 & 0 \\ k_{21}^{-} & \diamond & (N-1)k_{12}^{+}c_1^{\eta} & 0 & 0 & 0 \\ 0 & 2k_{21}^{-} & \diamond & (N-2)k_{12}^{+}c_2^{\eta} & 0 & 0 \\ & & & \ddots & & \\ 0 & 0 & 0 & (N-1)k_{21}^{-} & \diamond & k_{12}^{+}c_{N-1}^{\eta} \\ 0 & 0 & 0 & 0 & Nk_{21}^{-} & \diamond \end{pmatrix}, \tag{3}$$

where q_{ij} is the transition rate from state i to state j and the diamonds ($\diamond$) indicate a diagonal entry leading to a row sum of zero. Notice that the transition rates from state i to state j are scaled by the number of channels in state i. The upper diagonal elements are transitions mediated by $[Ca^{2+}]$ and use the bimolecular rate constants. The lower diagonal elements are independent of $[Ca^{2+}]$ and use unimolecular rate constants.

2.3 Dynamics of domain Ca^{2+}

This model is built under the assumption of instantaneous coupling, meaning that the time-scale for the change in the $[Ca^{2+}]$ in the domains is fast compared to the gating of the channels. The domains are coupled to the bulk compartments via the fluxes J_{cyt} and J_{er} given by

$$J_{cyt} = v_{cyt}\left(c_{cyt}^{d} - c_{cyt}\right) \tag{4}$$

$$J_{er} = v_{er}\left(c_{er} - c_{er}^{d}\right) \tag{5}$$

where c_{cyt}^{d} and c_{er}^{d} are the cytosolic and luminal domain Ca^{2+} concentrations, v_{cyt} is the rate of cytosolic domain collapse and v_{er} is the rate of luminal domain recovery [5].

The release of Ca^{2+} through IP_3Rs (J_{rel}) is given by

$$J_{rel} = \gamma\, v_{rel} \left(c_{er}^d - c_{cyt}^d\right) \tag{6}$$

where γ indicates the fraction of channels at the Ca^{2+} release site that are open and takes the values

$$\gamma \in \left\{0, \frac{1}{N}, \frac{2}{N}, \cdots, \frac{N-1}{N}, 1\right\}.$$

The release flux J_{rel} is thus proportional to the maximum conductance of the release site (v_{rel}), and the driving force is given by the difference between the luminal and cytosolic domain Ca^{2+} concentrations.

Based on Eqs. 4–6, the concentration balance equations for the domain Ca^{2+} concentrations are given by

$$\frac{dc_{cyt}^d}{dt} = \frac{1}{\lambda_{cyt}^d}\left(J_{rel} - J_{cyt}\right) \tag{7}$$

$$\frac{dc_{er}^d}{dt} = \frac{1}{\lambda_{er}^d}\left(-J_{rel} + J_{er}\right) \tag{8}$$

where λ_{er}^d and λ_{cyt}^d are scaling factors that account for the domain volumes.

Under the assumption of instantaneous coupling, the steady-state cytosolic and luminal domain Ca^{2+} concentrations are given as functions of γ and are found by setting the left hand sides of Eqs. 7 and 8 to zero, with the following result [11],

$$c_{cyt}^{d,ss}(n) = \frac{v_{cyt}}{v_{cyt} + v'_{er}} c_{cyt} + \frac{v'_{er}}{v_{cyt} + v'_{er}} c_{er} \tag{9}$$

$$c_{er}^{d,ss}(n) = \frac{v'_{cyt}}{v'_{cyt} + v_{er}} c_{cyt} + \frac{v_{er}}{v'_{cyt} + v_{er}} c_{er} \tag{10}$$

where

$$v'_{cyt} = \frac{\gamma v_{rel} v_{cyt}}{\gamma v_{rel} + v_{cyt}}, \qquad v'_{er} = \frac{\gamma v_{rel} v_{er}}{\gamma v_{rel} + v_{er}}, \qquad \text{and} \qquad \gamma = \frac{n}{N}.$$

We define the values of c_n in Eq. 3 in the previous section as

$$c_n = c_{cyt}^{d,ss}(n). \tag{11}$$

Thus, for any given c_{cyt} and c_{er} we have a generator matrix $Q(c_{cyt}, c_{er})$ and the time-evolution of the probability distribution of the number of open channels that can be found by solving the ODE initial value problem

$$\frac{d\boldsymbol{\pi}}{dt} = \boldsymbol{\pi} Q \tag{12}$$

where $\boldsymbol{\pi} = (\pi_0, \pi_1, \cdots, \pi_N)$, $\pi_i(t)$ is the probability of finding a release site in state i, and $\boldsymbol{\pi}(0)$ is the initial condition.

2.4 Ca^{2+} concentration balance equations

By considering the limit as the total number of release sites approaches infinity, we can study the Ca^{2+} handling in a whole cell model. The bulk Ca^{2+} concentrations are affected by the SERCA pumps (J_{pump}), a passive leak from the ER to the cytosol that is independent of release site activity (J_{leak}), and the total flux through the release sites (J^T_{rel}). These fluxes take the form,

$$J_{pump} = \frac{v_{pump}(c_{cyt})^2}{(k_{pump})^2 + (c_{cyt})^2}. \tag{13}$$

$$J_{leak} = v_{leak}\left(c_{er} - c_{cyt}\right) \tag{14}$$

$$J^T_{rel} = \sum_{n=0}^{N} \pi_n \gamma v^T_{rel} \left[c^{d,ss}_{er}(n) - c^{d,ss}_{cyt}(n)\right] \tag{15}$$

We define the total cytosolic and luminal Ca^{2+} concentrations as a the sum of the bulk concentration and the concentration in the domains scaled by the relative effective volumes, Λ^d_{cyt} and Λ^d_{er},

$$\hat{c}_{cyt} = c_{cyt} + \Lambda^d_{cyt}\bar{c}^d_{cyt} \tag{16}$$

$$\hat{c}_{er} = c_{er} + \frac{\Lambda^d_{er}}{\lambda_{er}}\bar{c}^d_{er}, \tag{17}$$

where $\bar{c}^d_{cyt} = \sum_{n=0}^{N} \pi_n c^{d,ss}_{cyt}(n)$ and $\bar{c}^d_{er} = \sum_{n=0}^{N} \pi_n c^{d,ss}_{er}(n)$ are average values for domain $[Ca^{2+}]$.

For a closed cell with no fluxes across the plasma membrane, it can be shown without approximation that $\hat{c}_{cyt}$ and $\hat{c}_{er}$ solve

$$\frac{d\hat{c}_{cyt}}{dt} = J^T_{rel} + J_{leak} - J_{pump} \tag{18}$$

$$\frac{d\hat{c}_{er}}{dt} = \frac{1}{\lambda_{er}}\left(-J^T_{rel} - J_{leak} + J_{pump}\right) \tag{19}$$

where J^T_{rel}, J_{leak}, and J_{pump} are given by Eqs. 15–13. Note that the fluxes that occur in Eqs. 18–19 are functions of c_{cyt} and c_{er} that must be evaluated using the values of $\hat{c}_{cyt}$ and $\hat{c}_{er}$ that are found by inverting

$$\hat{c}_{cyt} = c_{cyt} + \Lambda^d_{cyt} \sum_{n=0}^{N} \left[\pi_n \left(\frac{v_{cyt}}{v_{cyt} + v'_{er}} c_{cyt} + \frac{v'_{er}}{v_{cyt} + v'_{er}} c_{er}\right)\right] \tag{20}$$

$$\hat{c}_{er} = c_{er} + \frac{\Lambda^d_{er}}{\lambda_{er}} \sum_{n=0}^{N} \left[\pi_n \left(\frac{v'_{cyt}}{v'_{cyt} + v_{er}} c_{cyt} + \frac{v_{er}}{v'_{cyt} + v_{er}} c_{er}\right)\right]. \tag{21}$$

Eqs. 20 and 21 can be derived by combining Eqs. 16 and 17 with Eqs. 9 and 10 and using the definitions of $\bar{c}^d_{cyt}$ and $\bar{c}^d_{er}$.

Rearranging Eqs. 20–21 gives

$$\hat{c}_{cyt} = a_{11} c_{cyt} + a_{12} c_{er} \tag{22}$$

$$\hat{c}_{er} = a_{21} c_{cyt} + a_{22} c_{er} \tag{23}$$

where

$$a_{11} = 1 + \Lambda^d_{cyt} \sum_{n=0}^{N} \left(\pi_n \frac{v_{cyt}}{v_{cyt} + v'_{er}} \right) \tag{24}$$

$$a_{12} = \Lambda^d_{cyt} \sum_{n=0}^{N} \left(\pi_n \frac{v'_{er}}{v_{cyt} + v'_{er}} \right) \tag{25}$$

$$a_{21} = \frac{\Lambda^d_{er}}{\lambda_{er}} \sum_{n=0}^{N} \left(\pi_n \frac{v'_{cyt}}{v'_{cyt} + v_{er}} \right) \tag{26}$$

$$a_{22} = 1 + \frac{\Lambda^d_{er}}{\lambda_{er}} \sum_{n=0}^{N} \left(\pi_n \frac{v_{er}}{v'_{cyt} + v_{er}} \right). \tag{27}$$

Using Cramer's rule we see

$$c_{cyt} = \frac{a_{22}\hat{c}_{cyt} - a_{12}\hat{c}_{er}}{D} \qquad c_{er} = \frac{a_{11}\hat{c}_{er} - a_{21}\hat{c}_{cyt}}{D} \tag{28}$$

where $D = a_{11}a_{22} - a_{12}a_{21}$. In this manner, the fluxes J_{leak}, J_{pump}, and J^T_{rel} can then be evaluated as functions of $\hat{c}_{cyt}$ and $\hat{c}_{er}$. We now have a complete set of ODEs describing the behavior of the system on several spatial scales. Unlike previous models, this hybrid model of local and global Ca^{2+} signaling accounts for both release site dynamics and whole cell Ca^{2+} homeostasis.

The experimental studies we intend to simulate here used permeabilized cardiac myocytes. Permeabilizing the plasma membrane effectively clamps the cytosolic Ca^{2+} concentration to the level of the extracellular medium. Even in intact cells, fluxes across the plasma membrane can cause changes in total whole cell Ca^{2+} concentrations. In order to model these conditions, we included plasma membrane fluxes and allow the total Ca^{2+} in the cell to change. The flux of Ca^{2+} out of the cell is assumed to be proportional to the cytosolic [Ca^{2+}],

$$J_{out} = k_{out} c_{cyt} \tag{29}$$

where k_{out} is the extrusion rate constant. The inward Ca^{2+} flux, J_{in}, is assumed constant and independent of cytosolic [Ca^{2+}]. At steady state, J_{in} and J_{out} are equal, which means that

$$c^{ss}_{cyt} = \frac{J_{in}}{k_{out}}. \tag{30}$$

Because the steady state cytosolic [Ca^{2+}] is known from experiment, we use Eq. 30 to determine J_{in} consistent with the known c^{ss}_{cyt}. Varying k_{out} thus changes the magnitude of the plasma membrane fluxes without altering the steady-state cytosolic Ca^{2+} concentration. A low value of k_{out} corresponds to an intact cell; a high k_{out} reflects the conditions of a permeabilized cell.

2.5 Numerical Analysis and Contributions

MATLAB's ODE solvers were used to numerically integrate the set of ODEs presented in Sections 2.3 and 2.4 (for representative code, see Appendix). Studies focused on either the steady state behavior of the probability distribution ($\boldsymbol{\pi}$) and bulk Ca^{2+} concentrations (c_{cyt} and c_{er}) as a function of one or, alternatively, more parameters or the transient behavior for a given parameter set. The code for the matrix analytic method of calculating the expected spark duration was provided by Jeff Groff (see [2]). All simulations and parameter studies presented as figures or tables in the following sections are original work, as well as many others that are not presented for the sake of brevity.

3 Results

3.1 Parameter scan over the activation rate constant k_{12}^{+}

As discussed in the Introduction, the hybrid model of local and global Ca^{2+} signaling that is the focus of this thesis is designed to explore the effect of the addition of tetracaine (a pharmacological agent that reduces the single RyR open probability) on stochastic Ca^{2+} release by clusters of RyRs and whole cell Ca^{2+} homeostasis. Because there is evidence that tetracaine decreases the open probability of RyRs by increasing the mean closed dwell time of these intracellular Ca^{2+} channels ($\tau_C = 1/k_{12}^{+}c^{\eta}$), the primary parameter under consideration is k_{12}^{+} (see Eq. 1) . Decreasing this parameter corresponds to the effects of the addition of tetracaine (i.e., reducing the single RyR open probability). We examined the effect of changing k_{12}^{+} on the faction of open channels and the expected value of the spark duration. We also calculated the spark *Score*, a measure of the tendency of a system to spark, which is given by

$$Score = \frac{1}{N}\frac{Var[N_O]}{E[N_O]} \tag{31}$$

where N_O is the number of open channels in the Ca^{2+} release site model. The value of the *Score* ranges from 0 to 1; a *Score* of 0.2 or higher indicates a system with frequent or robust sparks [12]. For purposes of duration calculation, a spark is defined as starting when the release site reaches a threshold number of open channels ($N_O = \kappa = 5$ out of 10 channels) and ending when all the channels close ($N_O = 0$). The spark duration statistics were numerically calculated using the matrix analytic method described in [2] and are only reported when the *Score* was greater than 0.2. Finally, the fraction of open channels in a release site is given by

$$f_O = \frac{E[N_O]}{N}. \tag{32}$$

Fig. 2 summarizes these four measures as a function of the single channel Ca^{2+} activation rate constant k_{12}^{+}. The fraction of open channels at release sites increases with k_{12}^{+}, consistent with the effect of tetracaine on single channels. As the open probability decreases, the total $[Ca^{2+}]$ in the ER at steady state increases. Since the flux of the SERCA pumps (Eq. 13) is independent of the luminal $[Ca^{2+}]$, reducing the RyR open probability decreases (from right to left), the release flux (Eq. 15) while the flux into the ER stays constant. Although the

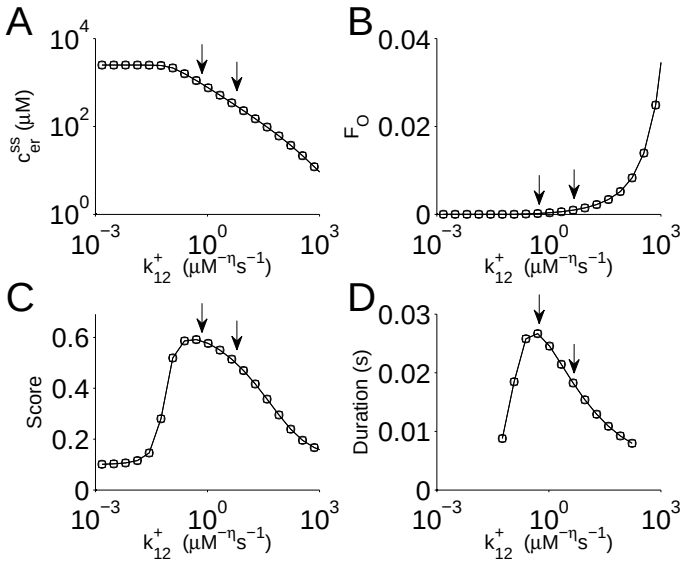

Figure 2: Release site dynamics and whole cell conditions at steady state as functions of the RyR activation rate constant k_{12}^+. A. Luminal Ca^{2+} concentration. B. Fraction of open channels. C. *Score*. D. Expected spark duration. The arrow on the right indicates the standard conditions; the left arrow designates the reduction in k_{12}^+ corresponding to the addition of tetracaine. All other parameter values as in Table 2.

greater difference between the luminal and cytosolic Ca^{2+} concentrations makes the passive leak term higher (Eq. 14), it is not enough to compensate for the decreased flux through the release site.

In the region where c_{er}^{ss} is somewhat elevated but k_{12}^+ is not low enough to shut down all channel activity, we see an increase in both the *Score* and the expected spark duration. Note that the increase in *Score* does not necessarily correspond to an increase in the frequency of sparks. Fewer but longer sparks can also can an increase in the *Score*. Consistent with experiment, we find that decreasing k_{12}^+ can lead to longer sparks driven by an overloaded ER [8].

The right arrow in each figure indicates the standard parameter set (see Table 2). The left arrow shows the k_{12}^+ value that corresponds to the conditions in the cell after the addition of tetracaine, $k_{12}^+ = 0.5\ \mu\text{M}^{-2}s^{-1}$. Experimentally, the addition of 0.7 mM of tetracaine caused an 88% reduction in open probability in lipid bilayer single channel recordings [8]. The reduction in k_{12}^+ chosen to represent the application of tetracaine show a similar reduction in P_O compared to the standard parameters, using

$$P_O = \frac{k_{12}^+ (c_{cyt}^{ss})^\eta}{k_{12}^+ (c_{cyt}^{ss})^\eta + k_{21}^-}. \tag{33}$$

Note that with this change in k_{12}^+, the fraction of open channels in the release site is only reduced by 79%, indicating that the interaction between the channels attenuates the decrease in channel activity occuring during the simulated application of tetracaine. Presumably, high luminal $[Ca^{2+}]$ provides the driving force for this Ca^{2+}-mediated channel coupling.

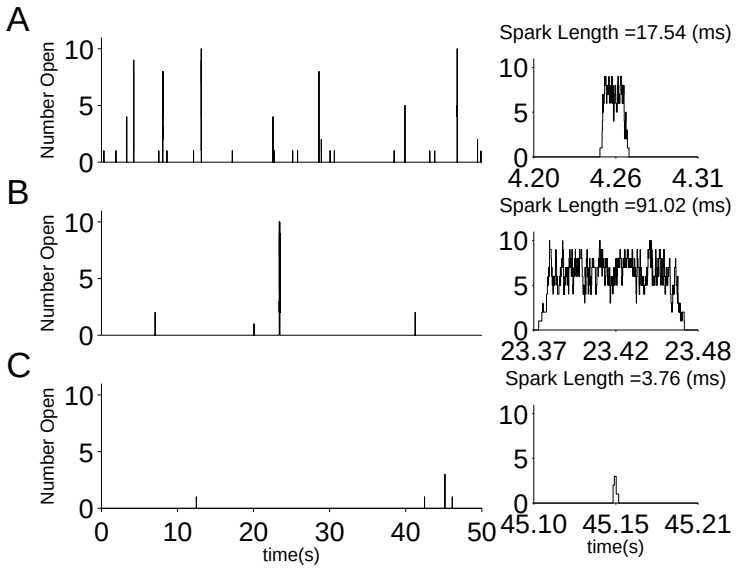

Figure 3: Gillespie simulations of sparks under three different steady state conditions. The left portion shows a 50 second simulation for a release site with $N = 10$ channels. The first release event with more than 5 open channels is shown on a larger scale on the right. Except where noted, all parameters values are as in Table 2. A: Standard parameters with $k_{12}^{+} = 4.5$ $\mu\text{M}^{-2}s^{-1}$ resulting $Score = 0.51$. B: Activation coefficient reduction with homeostasis: $k_{12}^{+} = 0.5$ $\mu\text{M}^{-2}s^{-1}$. $Score = 0.59$. C: Activation coefficient reduction without homeostasis $c_{er}^{fixed} = 342$ μM, $k_{12}^{+} = 0.5$ $\mu\text{M}^{-2}s^{-1}$, $Score = 0.11$.

3.2 Stochastic simulations of individual release sites

For any given parameter set, a simulation can be run to obtain an example of how a given release site might activate and inactivate in a stochastic fashion. Fig. 3 shows simulations generated by the Gillespie method [13] for the two values of k_{12}^{+} indicated in Fig. 2 and discussed. On the left is a simulation run for 50 seconds; on the right is a larger view of the first spark with a number of open channels above the threshold ($\kappa = 5$ channels). Fig. 3A shows the high frequency of sparks that characterizes the standard conditions. In this case, we see five sparks and multiple smaller release events with amplitudes below the threshold number of channels, which are referred to as Ca^{2+} quarks in the experimental literature. The expectated value of the spark duration is 18.3 ms; the first spark in this simulation has a duration of 17.5 ms.

When we change to the parameter set corresponding to the addition of tetracaine, the spark frequency is significantly reduced (Fig. 3B). Although there are fewer sparks, the variation in the number of open channels increases enough to raise the *Score*. In this simulation, there is one spark and three quarks. While the expected spark duration is 26.8 ms, sparks of 90 ms or more are not infrequent using the tetracaine parameter set, though they almost never occur with the standard parameter set. This is consistent with experimental observations: not all release events are long duration sparks; many are of the length seen before the addition of tetracaine [8].

In order to study the effect of the Ca^{2+} homeostasis mechanisms of the model, we can fix c_{er} and c_{cyt} to the values obtained with the standard parameters, then reduce k_{12}^{+} without

allowing the bulk Ca^{2+} concentrations to change, and compare these calculations to the results obtained when the bulk Ca^{2+} concentrations respond to Ca^{2+} release via spontaneous sparks. Fig. 3C shows that such a simulation results in only a few release events, none with more than three channels open. We therefore conclude that the homeostasis mechanisms have a significant impact on the hybrid model calculations and are required for the presence of prolonged sparks in this study. We also find that without an elevated luminal $[Ca^{2+}]$, a reduction in single channel open probability decreases spark frequency and does not cause an increase in spark duration. This is consistent with the experimental observations and qualitative explanations presented in Zima et al [8].

3.3 Transient effects of reduction of the activation rate constant

Because long duration sparks depend on an increased ER Ca^{2+} load, there is a period immediately after the addition of tetracaine when there are very few sparks, and those sparks which do occur have short durations [8, 9]. While steady-state dynamics were the focus of the previous parameter studies, we can use the steady state of the standard parameter calculation as the initial condition for the tetracaine parameter calculation and thereby simulate the transient dynamics observed upon the addition of tetracaine to permeabilized cardiac myocytes.

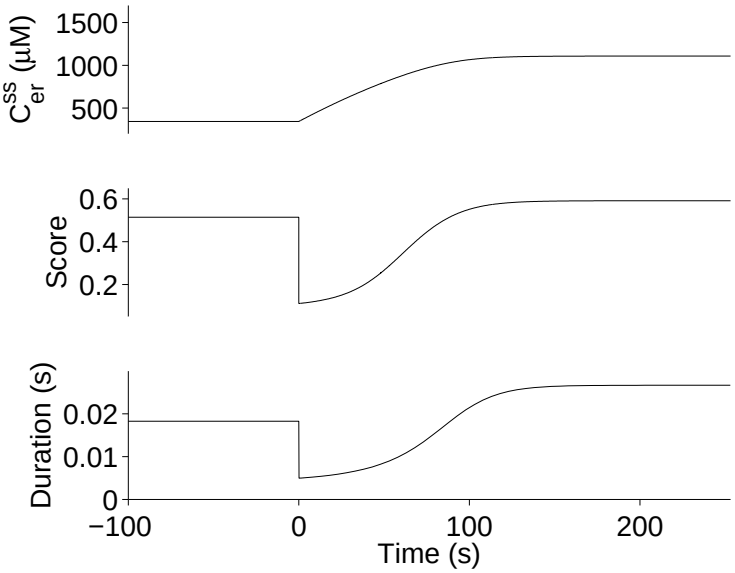

Figure 4: Transient effects of the reduction of the Ca^{2+}-activation rate constant k_{12}^{+}. At $t = 0$, k_{12}^{+} is reduced from 4.5 to 0.5 $\mu M^{-2}s^{-1}$. *Score* and expected spark duration are calculated as described in text. All other parameters as in Table 2.

As shown in Fig. 4, when the single channel open probability is reduced due to the simulated application of tetracaine, there is an initial decrease in both the expected spark duration and the *Score*. This decrease in stochastic Ca^{2+} release allows the ER to fill up, however, and both the *Score* and expected spark duration subsequently recover to greater than the original values. This is consistent with the experimentally observed suppression followed by activation of Ca^{2+} release after the addition of tetracaine and confirms that a high luminal $[Ca^{2+}]$ is a requirement for long sparks.

3.4 Two dimensional parameter scan

Flecainide has been shown to reduce the open probability of single channels by decreasing the dwell time in open states [10]. We therefore model the application of flecainide by increasing k_{21}^- rather than decreasing k_{12}^+ (see Eq. 1). Fig. 5 shows the response measures described above for a two dimensional scan over both parameters.

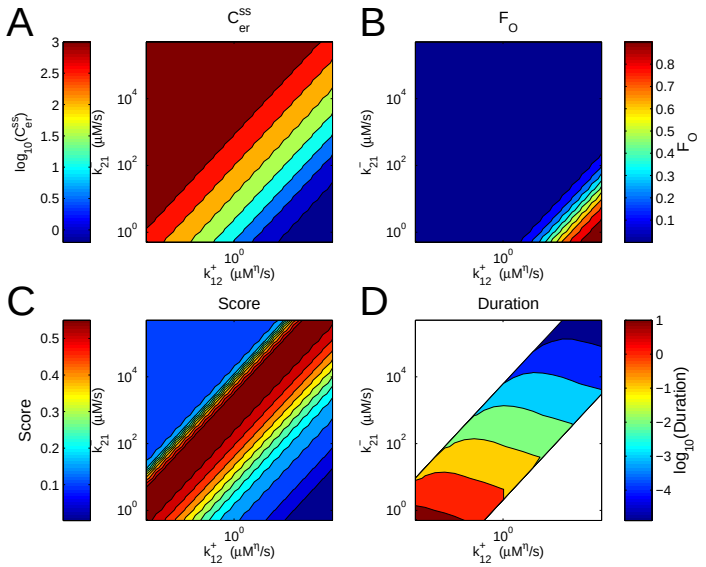

Figure 5: Release site dynamics and whole cell conditions as functions of the coefficient of activation and the deactivation rate. A. Luminal Ca^{2+} concentration. B. Fraction of open channels. C. *Score*. D. Expected spark duration. All other parameter values as in Table 2

The changes in the fraction of open channels are as expected upon changing k_{12}^+ and k_{21}^-; F_O is highest when k_{12}^+ is high and k_{21}^- is low. The luminal Ca^{2+} concentration is inversely proportional to the fraction of open channels, consistent with the earlier conclusion that decreasing the spark rate causes the ER to overload. The *Score* depends on the ratio between the two parameters rather than the magnitude of either one; for a given k_{12}^+ value, a corresponding k_{21}^- value can be found to yield a *Score* above 0.5. The range of high *Scores* indicates that the results seen in Fig. 2 do not require the particular k_{21}^- value chosen for the standard parameter set.

The expected duration, shown only for the range of values where the *Score* is greater than 0.2, decreases monotonically as k_{21}^- increases for any value of k_{12}^+. In contrast, as k_{12}^+ increases for a given k_{21}^- value, the expected duration first increases, then decreases. Once again we see that for any given value of k_{21}^-, we can find a range of values that produce the same qualitative effects as the addition of tetracaine.

Note that for a given ratio of k_{12}^+ to k_{21}^-, multiple steady solutions can be found that have the same c_{er}^{ss}, F_O, and *Score*, but differ with respect to the expected spark duration. When a single channel model with more than two states is used, we see a more complex variation in the *Score* and expected duration (not shown). However, the data in Figs. 2-4 shows that a simple two channel model in sufficient to reproduce the experimental results under consideration.

3.5 Mechanisms of RyR inhibition

Comparable reductions in the single channel open probability can be obtained by changing k_{12}^{+}, k_{21}^{-}, or both (see Fig. 5). Because of this, we can examine how different RyR inhibition mechanisms effect spark dynamics and whole cell Ca^{2+} homeostasis. Table 1 shows the steady state results of the standard parameter set, followed by three parameter changes that result in the same single channel P_O. As discussed in Sections 3.1 and 3.4, a reduction in k_{12}^{+} corresponds to the addition of tetracaine increasing RyR closed dwell times (B) and an increase in k_{21}^{-} is used to model the application of flecainide resulting in decreased open dwell times (C). Because there is disagreement about whether tetracaine also decreases open dwell times, an additional parameter set (D) is included that changes both parameters. For each of the three altered parameter sets the *Score*, luminal Ca^{2+} concentration, and F_O are the same. They differ only in the expected spark duration, which is consistent with the scaling seen in Fig. 5D. Comparison of these results to the response measures obtained with the standard parameters (A), suggests that prolonged spark duration upon addition of tetracaine may be interpreted as evidence for a mechanism of RyR inhibition that involves increasing the RyR closed dwell time without decreasing the open dwell time. Perhaps more importantly, Table 1 shows that it is not decreased P_O per se but rather the specific mechanism of RyR inhibition that determines whether spark duration decreases or increases upon ER overload.

	A. Standard Parameters	B. Tetracaine	C. Flecainide	D. Dual Mechanism
k_{12}^{+} ($\mu M^{-2}s^{-1}$)	4.5	0.5	4.5	1.5
k_{21}^{-} (s^{-1})	500	500	4500	1500
F_O	$9.6x10^{-4}$	$2.0x10^{-4}$	$2.0x10^{-4}$	$2.0x10^{-4}$
Score	0.51	0.59	0.59	0.59
c_{er}^{ss} (μM)	342	1112	1112	1112
Duration (ms)	18.2	26.7	2.97	8.90

Table 1: The effect of three mechanisms of RyR inhibition. Parameters sets B-D result in the same reduction in open probability and at steady state differ only in the expected spark duration.

As in Section 3.2, we present a stochastic simulation for each parameter set in Table 1. Fig. 6 reproduces the earlier results for the standard parameters (A) and the parameters corresponding to the application of tetracaine (B). Fig. 6C shows a simulation corresponding to the addition of flecainide, which results in nearly as many sparks as the standard conditions. However, as seen in both the representative spark (second column) and the expected spark duration (Table 1), the sparks are much shorter in duration. Fig. 6D shows the corresponding result when both k_{12}^{+} and k_{21}^{-} are changed. As might be expected from the previous two parameter sets, RyR inhibition by this dual mechanism shows a slight decrease in spark frequency and duration compared to the standard parameters, but less reduction than C or D.

Comparison of the luminal Ca^{2+} concentration for all three altered parameter sets with the standard conditions suggests that whole cell Ca^{2+} homeostasis can be dramatically affected by changes in release site dynamics due to RyR inhibition. While the specific mechanism of RyR inhibition can impact spark statistics such as the expected spark duration,

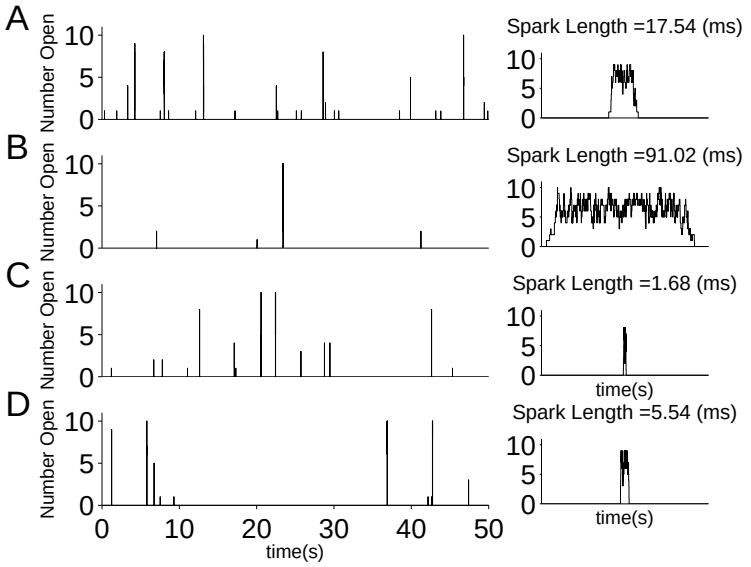

Figure 6: Gillespie simulations of sparks under four different steady-state conditions resulting from the parameter sets in Table 1. The left panels show 50 second simulations for release sites with $N = 10$ channels. The first release event of more than 5 channels is shown on a larger scale on the right. The parameters k_{12}^{+} and k_{21}^{-} are as in Table 1. All other parameters as in Table 2.

all three mechanisms have a similar impact on the whole cell Ca^{2+} homeostasis, i.e. the steady-state value of the ER Ca^{2+} concentration is increased. This somewhat unexpected result that different release site activity (Fig. 6B and C) can yield the same whole cell Ca^{2+} balance makes sense when one considers the fact that short duration sparks occurring at high frequency release the same amount of Ca^{2+} as long duration sparks occurring at low frequency.

4 Ongoing Research

There are still questions related to the current study that require consideration, such as what percentage of Ca^{2+} release is due to sparks and how much is due to the passive leak present when all RyRs are closed or to "hidden leak" in the form of quarks. The model also makes several assumptions, including instantaneous and mean-field coupling, the validity of which may need to be assessed in this context. Finally, the increased ER Ca^{2+} load seen with tetracaine has not yet been experimentally observed with the application of flecainide. Our model predicts elevated ER Ca^{2+} upon application of flecainide and thus awaits experimental confirmation. Further studies would be needed to determine if this could be effectively simulated.

The model above is very versatile and provides many options for future research. The single channel model presented above is the simplest possible model. Models with Ca^{2+}-dependent inactivation or luminal regulation have also been incorporated into the full model. Preliminary results indicate that when inactivation is included, results are qualitatively similar to those above, but with consistently shorter durations (not shown). For some parameter

Parameter	Definition	Value
λ_{er}	bulk ER effective volume fraction	1/6
Λ_{er}^{d}	total luminal domain effective volume fraction	1/30
Λ_{cyt}^{d}	total cytosolic domain effective volume fraction	1/30
v_{rel}^{T}	release flux rate	10 s^{-1}
v_{cyt}^{T}	cytosolic domain collapse rate	100 s^{-1}
v_{er}^{T}	luminal domain recovery rate	10 s^{-1}
v_{leak}	ER leak rate when all RyRs are closed	0.001 s^{-1}
v_{pump}	maximum SERCA pump rate	5 $\mu M s^{-1}$
k_{pump}	dissociation constant of SERCA pump	0.1 μM
η	cooperativity of Ca^{2+} binding to RyR	2
κ	threshold for spark duration calculation	5
N	number of channels per release site	10
k_{12}^{+}	association rate constant of activating Ca^{2+}	4.5 $\mu M^{-\eta} s^{-1}$
k_{21}^{-}	dissociation rate constant of activating Ca^{2+}	500 s^{-1}

Table 2: Standard parameters for the hybrid model of local and global Ca^{2+} signaling. Application of tetracaine is simulated by changing k_{12}^{+} from 4.5 to 0.5 $\mu M^{-\eta} s^{-1}$.

sets, oscillations in the luminal [Ca^{2+}] are observed, in spite of the fact that bulk cytosolic Ca^{2+} concentration is essentially "clamped" due to the permeabilized cell memebrane. There is much interest in luminal Ca^{2+} regulation of RyRs and the resulting effect on luminal Ca^{2+} oscillations observed in permeabilized cardiac myocytes in the laboratory of Sandor Györke (an experimental collaborator at OSU). Further work with variants of this hybrid model of local and global Ca^{2+} signaling could shed light on the mechanisms generating such oscillations.

5 Conclusion

Ca^{2+} signaling in cardiac myocytes occurs on multiple spatial and temporal scales. A hybrid Markov chain-ODE model was constructed to simultaneously account for whole cell Ca^{2+} homeostasis and local stochastic Ca^{2+} release site dynamics. Release sites were modeled as a collection of N instantaneously mean-field coupled intracellular Ca^{2+} channels, and their dynamics were incorporated into a whole cell model of Ca^{2+} homeostasis by assuming an infinite number of release sites. The model was used to analyze an experimental study in which application of tetracaine (a pharmacological agent that reduces single channel open probability of RyRs) was found to result in long duration Ca^{2+} sparks [8]. This modeling study reproduced this counter-intuitive result and supported the published suggestion that prolonged sparks are the result of increased ER load (Figs 2-3). We also generated predictions about the effect of other types of perturbations on the Ca^{2+} dynamics. We observed that the parameters corresponding to the addition of flecainide resulted in very short sparks (Table 1). Finally, we noted that similar whole cell Ca^{2+} balance can be obtained via radically different Ca^{2+} release site dynamics, as spark duration and spark frequency combine to determine the rate of Ca^{2+} release.

References

[1] JR Groff and GD Smith. Ryanodine receptor allosteric coupling and the dynamics of calcium sparks. Biophys. J., 95(1):135–154, 2008.

[2] JR Groff and GD Smith. Calcium-dependent inactivation and the dynamics of calcium puffs and sparks. J. Theor. Biol., 253(3):483–99, 2008.

[3] H DeRemigio and GD Smith. The dynamics of stochastic attrition viewed as an absorption time on a terminating Markov chain. Cell Calcium, 38(2):73–86, 2005.

[4] MA Huertas and GD Smith. The dynamics of luminal depletion and the stochastic gating of Ca^{2+}-activated Ca^{2+} channels and release sites. J. Theor. Biol., 246(2):332–354, 2007.

[5] J Keizer and L Levine. Ryanodine receptor adaptation and Ca^{2+}(-)induced Ca^{2+} release-dependent Ca^{2+} oscillations. Biophys J, 71(6):3477–3487, Dec 1996.

[6] GW De Young and J Keizer. A single-pool inositol 1,4,5-trisphosphate-receptor-based model for agonist-stimulated oscillations in Ca^{2+} concentration. Proc Natl Acad Sci USA, 89(20):9895–9, 1992.

[7] YX Li, J Keizer, SS Stojilkovic, and J Rinzel. Ca^{2+} excitability of the ER membrane: an explanation for IP_3-induced Ca^{2+} oscillations. Am J Physiol, 269(5 Pt 1):C1079–92, 1995.

[8] AV Zima, E Picht, DM Bers, and LA Blatter. Partial inhibition of sarcoplasmic reticulum ca release evokes long-lasting calcium release events in ventricular myocytes: role of luminal calcium in termination of calcium release. Biophysical Journal, 94(5):1867–79, Mar 2008.

[9] S Györke, V Lukyanenko, and I Györke. Dual effects of tetracaine on spontaneous calcium release in rat ventricular myocytes. Journal of Physiology, 500:297–309, 1997.

[10] H Watanabe, N Chopra, D Laver, HS Hwang, SS Davies, DE Roach, HJ Duff, DM Roden, AAM Wilde, and BC Knollmann. Flecainide prevents catecholaminergic polymorphic ventricular tachycardia in mice and humans. Manuscript in press courtesy of BC Knollmann.

[11] GSB Williams, EJ Molinelli, and GD Smith. Modeling local and global intracellular calcium responses mediated by diffusely distributed inositol 1,4,5-trisphosphate receptors. J. Theor. Biol., 253(1):170–188, 2008.

[12] V Nguyen, R Mathias, and GD Smith. A stochastic automata network descriptor for markov chain models of instantaneously-coupled intracellular Ca^{2+} channels. Bull. Math. Biol., 67(3):393–432, 2005.

[13] Daniel T Gillespie. A general method for numerically simulating the stochastic time evolution of coupled chemical reactions. Journal of Computational Physics, 22:403–34, Dec 1976.

Appendix: Representative Matlab code

The following code was used to generate Fig. 2. The program `parameter_scan` generated the data using the internal MATLAB ODE solver `ode15s` which calls `concentration_equations`, the file that defines the differential equations to be numerically integrated. The file `figures` was used to create the figure itself. The other scripts are subroutines called in `parameter_scan`. The subroutines `ballbin`, `expandedKmeanfield`, `meanstdfromdist`, and `qballbin2` were available to the lab from prior research. The code `matrixAnalyticPuffStats` was provided by Jeff Groff (see [2]). All other code is original work.

parameter_scan

```
% Runs a parameter scan over k12+ for a two state (CO) or three state (COI)
% model.  Returns information on steady state calcium concentrations and
% release site statistics.  Each parameter set is run through an ODE solver
% until a specified steady state is reached.

clear
clc

% FLAGS

CellType = 1; % 0=closed, 1=open
Inactivation = 0; % 0=NoInact, 1=fast, 2=slow

FileName = 'OpenCellNoInact.mat';

NumChannels = 10; % Number of channels per release site
kappa = 5;        % Threshold of duration calculations
C_cyt_hat0 = .1;  % Initial cytosolic [Ca] (uM)
C_er_hat0 = 500;  % Initial ER [Ca] (uM)
a = logspace(-1,0,2); % scaling factor for paramter scan

steady_state_tolerance = 1e-5;

global Q

%Build Model

k12p = 1.5e2;  % uM^-eta s^-1
k21m = 0.5e2;  % 1/s

if (Inactivation == 0)      %no inactivation
    k23p = 0; %uM^-eta s^-1
    k32m = 0; %1/s
elseif (Inactivation == 1)  %fast inactivation
```

```
    k23p = .015e3; %uM^-eta s^-1
    k32m = .005e3; %1/s
else                          %slow inactivation
    k23p = .0015e3; %uM^-eta s^-1
    k32m = .0005e3; %1/s
end

Kp1         = [ 0 k12p 0; 0 0 k23p; 0 0 0 ];
Km1         = [ 0 0 0; k21m 0 0; 0 k32m 0 ];

[ SingleChannelStates, dummy ] = size(Kp1);

b = ballbin(NumChannels,SingleChannelStates);
Qbb = qballbin2(b);
NumStates = length(b);

KpN = expandedKmeanfield(Kp1,Qbb,b);
KmN = expandedKmeanfield(Km1,Qbb,b);

% Define Parameters
vT_rel       = 10;  %1/s
vT_cyt       = 100; %1/s
vT_er        = 10;  %1/s
eta          = 2;
v_leak       = 0.001;   %1/s
v_pump       = 5;       %uM/s
k_pump       = .1;      %uM
lambda_er    = 1/6;
LambdaD_cyt  = 1/30;
LambdaD_er   = 1/30;
Cbin         = 2;     %open (Ca releasing) state
C_cyt_ss_det = .1;   %uM
k_out        = 10000; %1/s

n_index_channels = 0:NumChannels;
n_open_by_state = b(:,Cbin)';

p=zeros(size(KpN));

p(1) =  NumChannels;
p(2) =  NumStates;
p(3) =  vT_rel;
p(4) =  vT_cyt;
p(5) =  vT_er;
p(6) =  eta;
p(7) =  v_leak;
```

```
p(8) =  v_pump;
p(9) =  k_pump;
p(10) = lambda_er;
p(11) = LambdaD_cyt;
p(12) = LambdaD_er;
p(13) = Cbin; %open (Ca releasing) state
p(14) = CellType;
if (CellType == 1)
    p(15) = C_cyt_ss_det;
    p(16) = k_out;
else
    p(15) = 0;
    p(16) = 0;
end
p(17:NumStates+16) =  n_open_by_state;

P = cat(3,KpN,KmN,p);

% Define initial conditions
pi0 = [1 zeros(1,(NumStates-1))]; % All channels closed

%Initialize matrices for scan results
C_cyt_ss = zeros(2,length(a)); C_er_ss = zeros(2,length(a));
Score = zeros(2,length(a)); MaxScore = zeros(2,length(a));
Duration = zeros(2,length(a)); DurDistribution = zeros(2,1000,length(a));
ExpectedOpen = zeros(2,length(a)); CV = zeros(2,length(a));
Po = zeros(2,length(a)); Fo = zeros(2,length(a));
PI_N_Open = zeros(1,NumChannels+1);

for loop=1:2
    for j = 1:length(a)

        %Redefine k12p based on a, run ODE solver to determine ss
        k12pa = a(j)*k12p; Kp1 = [ 0 k12pa 0; 0 0 k23p; 0 0 0 ];
        P(:,:,1)=expandedKmeanfield(Kp1,Qbb,b);

        odetime = 200; odetime_add=50;
        [T,Y] = ode15s(@concentration_equations,[0 odetime], ...
            [pi0 C_cyt_hat0 C_er_hat0],[],[P]);

        deltaC_cyt = (Y(end-1,(NumStates+1)) - Y((end-3),(NumStates+1)))/2;
        deltaC_er = (Y(end-1,(NumStates+2)) - Y((end-3),(NumStates+2)))/2;

        figure(1) %Plot [Ca] while ODE is running
        subplot(2,1,1)  %C_er_hat
        plot(T,Y(:,(NumStates+2)),'o-');
```

```
ylabel('C_{er}^{hat}')
xlabel('time')

subplot(2,1,2)  %C_cyt_hat
plot(T,Y(:,(NumStates+1)),'ro-');
ylabel('C_{cyt}^{hat}')
xlabel('time')

%run ode until steady state tolerance is reachced
while (abs(deltaC_er)>steady_state_tolerance) && ...
        (Y(end,NumStates+2) < 10000)
    odetime = odetime + odetime_add;
    [T_add,Y_add] = ode15s(@concentration_equations,...
        [T(end) odetime],[Y(end,:)],[],[P]);
    T =[T; T_add(2:end)];
    Y =[Y; Y_add((2:end),:)];
    deltaC_cyt=(Y(end-1,(NumStates+1))-Y((end-3),(NumStates+1)))/2;
    deltaC_er=(Y(end-1,(NumStates+2))-Y((end-3),(NumStates+2)))/2;

    figure(1)
    subplot(2,1,1)  %C_cyt_hat
    plot(T,Y(:,(NumStates+2)),'o-');
    ylabel('C_{er}^{hat}')
    xlabel('time')

    subplot(2,1,2)  %C_cyt_hat
    plot(T,Y(:,(NumStates+1)),'ro-');
    ylabel('C_{cyt}^{hat}')
    xlabel('time')

end

%Calculate and Record Scores
Score_time = TimeStats(Y,NumStates,n_open_by_state,NumChannels);

MaxScore(loop,j) = max(Score_time);
Score(loop,j) = Score_time(end)

PI_States_ss = Y(end,1:NumStates);
C_cyt_hat_ss = Y(end,(NumStates+1));
C_er_hat_ss = Y(end,(NumStates+2));

%Convert from C_cyt_hat to C_cyt
gamma = n_open_by_state./NumChannels;

v_cyt2 = (gamma*vT_rel*vT_cyt)./(gamma*vT_rel + vT_cyt);
```

```
    v_er2 = (gamma*vT_rel*vT_er)./(gamma*vT_rel + vT_er);

    a11 = 1 + LambdaD_cyt*sum(PI_States_ss*vT_cyt./(vT_cyt+v_er2));
    a12 = LambdaD_cyt*sum(PI_States_ss.*v_er2./(vT_cyt + v_er2));
    a21 = (LambdaD_er/lambda_er)*...
        sum(PI_States_ss.*v_cyt2./(v_cyt2+vT_er));
    a22 = 1 + (LambdaD_er/lambda_er)*...
        sum(PI_States_ss*vT_er./(v_cyt2 + vT_er));

    C_cyt_ss(loop,j) = (a22*C_cyt_hat_ss - a12*C_er_hat_ss)/...
        (a11*a22 - a12*a21);
    C_er_ss(loop,j) = (a11*C_er_hat_ss - a21*C_cyt_hat_ss)/...
        (a11*a22 - a12*a21);

    % Calculate PI vector for number of open channels and open
    % probability of a single channel

    % find states with i open channels, then calculate the total
    % probability of i open channels
    for i = 0:NumChannels
        openstates = find(b(:,Cbin)==i);
        PI_N_Open(1,i+1) = sum(Y(end,openstates));
    end

    ExpectedOpen(loop,j) = sum(PI_States_ss.*n_open_by_state)
    Fo(loop,j) = ExpectedOpen(loop,j)/NumChannels
    Po(loop,j)= (k12pa*(C_cyt_ss(loop,j)^eta))/...
        (k12pa*(C_cyt_ss(loop,j)^eta) + k21m)

    %Calculate Spark Duration
    if (Score(loop,j) < .2)
        Duration(loop,j)=0
    else
        calcdist = 1;
        x = linspace(0,1,1000);
        [EPD,varPD,f] = matrixAnalyticPuffStats(Q,PI_States_ss,b,...
            Cbin,kappa,calcdist,x);
        Duration(loop,j) = EPD
        DurDistribution(loop,:,j)=f;
        [mu,sigma] = meanstdfromdist(x,f)
        CV(loop,j) = sigma/mu
    end
end

%Redefine starting conditions for loop 2
pi0 = [zeros(1,NumStates)];
```

```
    pi0(find(b(:,Cbin)==NumChannels)) = 1; % All channels open
end

save(FileName);
```

concentration_equations

```
% Defines the ODEs to be called by parameter_scan

function dY = concentration_equations(t,Y,P)

global Q

%parameters
KpN = P(:,:,1);
KmN = P(:,:,2);
p = P(:,:,3);

NumChannels     = p(1);
NumStates       = p(2);
vT_rel          = p(3);
vT_cyt          = p(4);
vT_er           = p(5);
eta             = p(6);
v_leak          = p(7);
v_pump          = p(8);
k_pump          = p(9);
lambda_er       = p(10);
LambdaD_cyt     = p(11);
LambdaD_er      = p(12);
Cbin            = p(13); %open (Ca releasing) site
CellType        = p(14); % 0=closed, 1=open
C_cyt_ss_det    = p(15);
k_out           = p(16);
n_open_by_state = p(17:NumStates+16);

% variables
PI = Y(1:NumStates)';
C_cyt_hat = Y(NumStates+1);
C_er_hat = Y(NumStates+2);

% equations and values defined
```

```
gamma = n_open_by_state./NumChannels;

v_cyt2 = (gamma*vT_rel*vT_cyt)./(gamma*vT_rel + vT_cyt);
v_er2 = (gamma*vT_rel*vT_er)./(gamma*vT_rel + vT_er);

a11 = 1 + LambdaD_cyt*sum(PI*vT_cyt./(vT_cyt+v_er2));
a12 = LambdaD_cyt*sum(PI.*v_er2./(vT_cyt + v_er2));
a21 = (LambdaD_er/lambda_er)*sum(PI.*v_cyt2./(v_cyt2+vT_er));
a22 = 1 + (LambdaD_er/lambda_er)*sum(PI*vT_er./(v_cyt2 + vT_er));

C_cyt = (a22*C_cyt_hat - a12*C_er_hat)/(a11*a22 - a12*a21);
C_er = (a11*C_er_hat - a21*C_cyt_hat)/(a11*a22 - a12*a21);

Cdss_cyt = vT_cyt*C_cyt./(vT_cyt+v_er2) + v_er2*C_er./(vT_cyt + v_er2);
Cdss_er = v_cyt2*C_cyt./(v_cyt2+vT_er) + vT_er*C_er./(v_cyt2 + vT_er);

%Q-Matrix formation

Cp1 = Cdss_cyt.^eta;
Cm1 = ones(1,NumStates);

CpN = diag(Cp1);
CmN = diag(Cm1);

CaKpN = CpN*KpN;
CaKmN = CmN*KmN;

CaKpN = CaKpN - diag(sum(CaKpN,2));
CaKmN = CaKmN - diag(sum(CaKmN,2));

Q = CaKpN + CaKmN;

J_leak = v_leak*(C_er - C_cyt);

J_pump = v_pump*(C_cyt^2)/((k_pump^2)+(C_cyt^2));

JT_rel = sum(PI.*gamma*vT_rel.*(Cdss_er-Cdss_cyt));

if (CellType == 1)
    J_out = k_out*C_cyt;

    J_in = k_out*C_cyt_ss_det;
end

%dif eqs defined
```

```
dY(1:NumStates) = PI*Q;  %dPI/dt

if (CellType == 0)
    dY(NumStates +1) = JT_rel + J_leak - J_pump; %dC_cyt_hat/dt
else
    dY(NumStates +1) = JT_rel + J_leak - J_pump + J_in - J_out;
end

dY(NumStates +2) = (1/lambda_er)*(-JT_rel - J_leak + J_pump); %dC_er_hat/dt

dY = dY';
```

ballbin

```
% BALLBIN returns all the possible ways B that NBALL indistinguishable
% balls can be placed in NBIN bins.  The NBIN cols of B represent bins;
% the rows of B are the ways.

function [ b ] = ballbin(nball,nbin)

if nbin == 1
   b = nball;
   return
end

if nball == 0
   b = zeros(1,nbin);
   return
end

b = [];
for bl = nball:-1:0
   [ br ] = ballbin(nball-bl,nbin-1);
   b = [ b; bl*ones(size(br,1),1) br ];
end

b = sparse(b);
return
```

expandedKmeanfield

```
% Generates mean field KN matrix with zeros on diagonals from a single
% channel model K1 matrix and using QBB, the output of qballbin2.

function [ KN ] = expandedKmeanfield(K1,Qbb,b)

[ M, dummy ] = size(K1);

[ a ] = find(Qbb ~= 0);
[ i, j ] = find(Qbb ~= 0);

fr = sub2ind(size(Qbb),i,j);
to = sub2ind(size(Qbb),j,i);

KN = zeros(size(Qbb));

KN(a)=b(sub2ind(size(b),i,Qbb(fr))).*K1(sub2ind(size(K1),Qbb(fr),Qbb(to)));

return
```

matrixAnalyticPuffStats

```
% Q - infinitesimal generator matrix
% stateSpace - state space result from ballbin
% iOpen - index of open state
% kappa - number of open channels at puff start

function [EPD,varPD,f] = matrixAnalyticPuffStats(Q,poeq,stateSpace,...
    iOpen,kappa,calcdist,x)

O0 = find(stateSpace(:,iOpen)==0);
O1 = find(stateSpace(:,iOpen)==1);
Ok = find(stateSpace(:,iOpen)==kappa);
Os = find(stateSpace(:,iOpen)~=0 & stateSpace(:,iOpen)~=1 & ...
    stateSpace(:,iOpen)~=kappa);

N0 = length(O0);
N1 = length(O1);
Nk = length(Ok);
Ns = length(Os);
```

```
Z0 = zeros(1,N0);
Z1 = zeros(1,N1);
Zk = zeros(1,Nk);
Zs = zeros(1,Ns);

newStateSpace = [O0; O1; Ok; Os];

Qnew = Q(:,newStateSpace); % rearrange columns
Qnew = Qnew(newStateSpace,:); % rearrange rows

a = [1 N0+1 N0+N1+1 N0+N1+Nk+1];
b = [N0 N0+N1 N0+N1+Nk N0+N1+Nk+Ns];

Q00 = Qnew(a(1):b(1),a(1):b(1));
Q01 = Qnew(a(1):b(1),a(2):b(2));
Q0k = Qnew(a(1):b(1),a(3):b(3));
Q0s = Qnew(a(1):b(1),a(4):b(4));

Q10 = Qnew(a(2):b(2),a(1):b(1));
Q11 = Qnew(a(2):b(2),a(2):b(2));
Q1k = Qnew(a(2):b(2),a(3):b(3));
Q1s = Qnew(a(2):b(2),a(4):b(4));

Qk0 = Qnew(a(3):b(3),a(1):b(1));
Qk1 = Qnew(a(3):b(3),a(2):b(2));
Qkk = Qnew(a(3):b(3),a(3):b(3));
Qks = Qnew(a(3):b(3),a(4):b(4));

Qs0 = Qnew(a(4):b(4),a(1):b(1));
Qs1 = Qnew(a(4):b(4),a(2):b(2));
Qsk = Qnew(a(4):b(4),a(3):b(3));
Qss = Qnew(a(4):b(4),a(4):b(4));

G01 = poeq(O0)*Q01;

QTTPS = [Q11 Q1s; Qs1 Qss];
QTAPS = [Q10 Q1k; Qs0 Qsk];
G00G0k = - [G01 Zs]*inv(QTTPS)*QTAPS;
G00 = G00G0k(1:N0);
G0k = G00G0k(N0+1:N0+Nk);

phik = G0k/sum(G0k);
phiPD = [Z1 phik Zs];

QTTPD = [Q11 Q1k Q1s; Qk1 Qkk Qks; Qs1 Qsk Qss];
```

```
QTAPD = [Q10; Qk0; Qs0];
invQTTPD = inv(QTTPD);

NT = N1+Nk+Ns;
unos = ones(NT,1);

EPD = -sum(phiPD*invQTTPD);
varPD = phiPD*(-invQTTPD)*(2*eye(NT) - unos*phiPD)*(-invQTTPD)*unos;

if calcdist == 1
    t = sum(QTTPD,2);
    f = zeros(size(x));
    for ii = 1:length(x)
        xnow = x(ii);
        f(ii) = - phiPD * (expm(xnow*QTTPD)) * t;
    end
else
    f = [];
end

return
```

meanstdfromdist

```
% Calculates the mean and standard deviation from a distribution.

function [mu,sigma] = meanstdfromdist(t,f)

shoudbeone = trapz(t,f);
mu = trapz(t,t.*f);
sm = trapz(t,t.^2.*f);
sigma = sqrt(sm-mu^2);

return
```

qballbin2

```
% QBALLBIN2 returns the SIZE(B,1) by SIZE(B,1) matrix Q(I,J) that
```

```
% (when nonzero) indicates the transitions required to make a B(I,:)
% to B(J,:) state change.  Q(I,J) is the bin that lost a ball.  Q(J,I)
% is the bin that gained a ball.

function [ q ] = qballbin2(b)

[ nconfig, nbin ] = size(b);

nnzcolb = length(b(:,1)); % nnz in a column of b (same for each col)
nnzq = nbin*(nbin-1)*nnzcolb; % nnz ultimately in q
q = spalloc(nconfig,nconfig,nnzq);
for i = 1:nbin
    ai = find(b(:,i)>0);
    for j = 1:nbin
        if i~=j
            aj = find(b(:,j)>0);
            q = q+sparse(ai,aj,i,nconfig,nconfig,nnzcolb);
        end
    end
end

return
```

TimeStats

```
% Calculates the Score as a function of time

function [ Score_time ] = TimeStats(Y, Numstates, n_open_by_state, NumChannels)

PI_time = Y(:,1:Numstates);
[DimY, DimN] = size(PI_time);
ScaleY = ones(DimY,1);
ScaleN = ones(1,DimN);
X = ScaleY*n_open_by_state;
E_time = sum((PI_time.*X),2);
E_time_expanded = E_time*ScaleN;
Var_time = sum((PI_time.*((X-E_time_expanded).^2)),2);
Score_time = (1/NumChannels)*(Var_time./E_time);
```

figures

```
% Prints results of a parameter scan generated using "parameter_scan.m"

% Plot C_er_ss vs k12p
subplot(2,2,1)
loglog((a*k12p),C_er_ss(1,:),'ko-');
ylabel('c_{er}^{ss} ({\mu}M)', 'FontSize',15);
xlabel('k_{12}^{+}  ({\mu}M^{-\eta}s^{-1})', 'FontSize',15);
hold on
loglog((a*k12p),C_er_ss(2,:),'ks-');
hold off
xlim([1e-3 1e3])
box off
set(gca,'fontsize',20)
set(gca,'Tickdir','out')
set(gca,'XTick',[1e-3 1e0 1e3])
annotation('arrow',[.305 .305], [.915 .865]);
annotation('arrow',[.35 .35], [.885 .835]);
set(gcf,'DefaulttextUnits','normalized')
set(gcf,'DefaulttextFontSize',30)
text(-.4,1.1,'A')

% Plot Fraction of Open Channels vs k12p
subplot(2,2,2)
semilogx((a*k12p),Fo(1,:),'ko-');
ylabel('F_{O}', 'FontSize',15);
xlabel('k_{12}^{+}  ({\mu}M^{-\eta}s^{-1})', 'FontSize',15);
hold on
semilogx((a*k12p),Fo(2,:),'ks-');
hold off
xlim([1e-3 1e3])
box off
set(gca,'fontsize',20)
set(gca,'Tickdir','out')
set(gca,'XTick',[1e-3 1e0 1e3])
annotation('arrow',[.74 .74], [.69 .64]);
annotation('arrow',[.785 .785], [.7 .65]);
text(-.4,1.1,'B')

% Plot Score vs k12p
subplot(2,2,3)
semilogx((a*k12p),Score(1,:),'ko-');
ylabel('Score', 'FontSize',15);
xlabel('k_{12}^{+}  ({\mu}M^{-\eta}s^{-1})', 'FontSize',15);
```

```
hold on
semilogx((a*k12p),Score(2,:),'ks-');
hold off
xlim([1e-3 1e3])
ylim([0 max(Score(1,:))+.1])
box off
set(gca,'fontsize',20)
set(gca,'Tickdir','out')
set(gca,'XTick',[1e-3 1e0 1e3])
annotation('arrow',[.305 .305], [.47 .42]);
annotation('arrow',[.35 .35], [.44 .39]);
text(-.4,1.1,'C')

% Plot Expected Duration vs k12p
none = find(Duration==0);
Duration(none) = NaN;
subplot(2,2,4)
semilogx((a*k12p),Duration(1,:),'ko-');
ylabel('Duration (s)', 'FontSize',15);
xlabel('k_{12}^{+}  ({\mu}M^{-\eta}s^{-1})', 'FontSize',15);
hold on
semilogx((a*k12p),Duration(2,:),'ks-');
hold off
xlim([1e-3 1e3])
box off
set(gca,'fontsize',20)
set(gca,'Tickdir','out')
set(gca,'XTick',[1e-3 1e0 1e3])
annotation('arrow',[.74 .74], [.485 .435]);
annotation('arrow',[.785 .785], [.4 .35]);
text(-.4,1.1,'D')

print(['Summary' ],'-deps2')
```